STUDIA UBB PHYSICA, Vol. 62 (LXII), 1-2, 2017, pp. 87-99
(RECOMMENDED CITATION)
doi:10.24193/subbphys.2017.08

MAGNETIC PROPERTIES OF THE PEROVSKITE OXIDE $PbV_{1-X}Fe_XO_3$ INVESTIGATED BY ELECTRON PARAMAGNETIC RESONANCE SPECTROSCOPY

A. OKOS[1], OANA RAITA[2], A. POP[1*]

ABSTRACT. The perovskite oxide $Pb(V_{1-x}Fe_x)O_3$ ($0 \leq x \leq 0.75$) was synthesised by solid state reaction under high pressure (HP) – high temperature (HT) conditions. The effect of partial substitution of V with Fe on magnetic properties of $PbVO_3$ compound were studied by Electron Paramagnetic Resonance (EPR) spectroscopy measurements.

***Keywords**: PbVO₃, high pressure - high temperature synthesis, EPR spectroscopy*

INTRODUCTION

The properties of ABO_3 perovskite oxides can often be improved by introducing magnetic dopants as long as their ferroelectric properties can be maintained.

Bulk $PbVO_3$ is known to be a $PbTiO_3$-type structure with a large tetragonal distortion (c/a = 1.22), with the V atoms displaced from symmetric O–V–O bonding along the c-axis, [1, 2].

[1] *Faculty of Physics, Babes-Bolyai University, Str. M Kogălniceanu, Nr. 1, RO-400084 Cluj-Napoca, Romania.*
[2] *INCDTIM, Str. Donath Nr. 65-103, RO-400293 Cluj-Napoca, Romania.*
[*] *Corresponding author: aurel.pop@phys.ubbcluj.ro*

Both theoretical and experimental studies have shown that V ions in bulk $PbVO_3$ are arranged in two-dimensional antiferromagnetic (AFM) ordering [3-5]. However, a long magnetic order is difficult to realize in $PbVO_3$ samples as it is often coupled to a spin glass phase.[1,6].

The single d electron per V^{IV} is localized and ordered into the xy orbital in the basal plane; the in-plane interatomic V–O–V interactions between the localized- electron spins give a broad maximum in the paramagnetic susceptibility near 200 K ,typical of 2D antiferromagnetic interactions [2,7].

If the weak magnetism is caused by the 2D arrangement of the V cations, the substitution could reduce the tendency of the system to form a 2D network and could lead to the onset of a 3D magnetic ordering.

The Fe ion with a large magnetic moment could provide some remnant magnetic moments at the oxygen ions and degrade the magnetic moment of the V ions by Fe–O –V super-exchange interaction [8].

The $PbV_{1/2}Fe_{1/2}O_3$ sample was previously synthesized at the pressure p = 7 GPa and temperature T = 800-1000° C, [9].The tetragonal distortion, which is still large in $PbV_{1/2}$ $Fe_{1/2}$ O_3 (the c/a = 1.18, placed between the values of 1.23 for $PbVO_3$ and 1.06 for $PbTiO_3$) is considered to be a second order Jahn-Teller effect caused by the electronic configuration of the V^{5+} ion and the lone electron pair of the Pb^{2+} ion.

In the present work, we will attempt to shed some light on the problem of the effect of partial substitution of V with Fe in of $PbVO_3$ compound on magnetic properties by Electron Paramagnetic Resonance (EPR) spectroscopy measurements.

EXPERIMENTAL

$PbV_{1-x}Fe_xO_3$ ($0 \leq x \leq 0.75$) polycrystalline samples were prepared by solid state reaction under high pressure, high temperature conditions (HP-HT) in a CONAC type apparatus.

For our samples almost single phase samples were obtained at pressures of 6 GPa and temperatures of 950° C, [10,11]. EDX measurements evidenced that the chemical composition of the samples with x < 0.5 were little different from those expected from starting elements.

For samples with x < 0.5 Fe the main phase correspond to the tetragonal structure in the space group P4mm. The a = b lattice constants do not depend on the composition and the unit cell height c decreased linearly with increasing iron content. [10]

X-Ray Absorption Spectroscopy (XAS) data for the vanadium K edge reveals in our samples the presence of V^{4+} and $V^{5+,}$ and below x=0.5 Fe the composition of the samples can be written as $Pb(V^{4+}_{1-2x}V^{5+}_xFe^{3+}_x)O_3$ [11]. For x = 0.5 all the V^{4+} cations are exhausted and consequently the sample contains only V^{5+} and Fe^{3+} cations (result consistent with the need / choice of starting oxides). This can also explain why the solid solution stops at x = 0.5.

Electron Paramagnetic Resonance (EPR) measurements were carried out on a Bruker Elexsys E500 spectrometer in X band (at 9.4 GHz) and in function of temperature.

RESULTS AND DISCUSSION

EPR was used as an effective tool to study the local magnetic interactions of Vanadium ions. EPR spectra of our $PbVO_3$ powder sample show a well-resolved hyperfine structure typical for V^{4+} ions , as in fig.11 and reference [11]. The EPR spectra of V(IV) ions in an isotropic environment exhibit eight lines of equal peak-to-peak width due to the hyperfine coupling of one unpaired electron (S =1/2) with the nuclear spin (I =7/2) of ^{51}V. The spectrum shows that both parallel and perpendicular features can be seen.

The EPR parameters for V^{4+} ions obtained from experimental spectra are consistent with a square–pyramidal C_{4v} coordination specific for vanadyl ions [11-16]. The hyperfine coupling constants $A_{||}$ and $A_{\perp}$ are sensitive to the local bonding environment for V^{4+} coordinated with oxygen ligands.

The small decrease of the hyperfine coupling $A_{||}$ and $A_{\perp}$ suggest the slight increase of ligand field with increasing temperature from 110K to 300K [11].

Three signals are invariably reported for Fe^{3+} [17-19]: a sharp line around *g*=4.3, interpreted as Fe^{3+} in a tetrahedral environment with strong rhombic distortion, a broad line around *g*=2.3 due to oxidic Fe species and a line around *g*=2, interpreted as Fe^{3+} in (distorted) octahedral environment

The widths of the line are larger in low magnetic fields when compared to high magnetic fields. If the lowest doublet, $|S\pm1/2>$ is populated, it gives a g value of 2 to 6 whereas if the middle Kramer's doublet $|S\pm3/2>$ is populated, a g value 4.30 is expected.

The Fe substitution samples investigated by EPR spectroscopy are x=25%Fe and x=40%Fe. Figure 1 shows the spectra for x=0.25 sample at 5 temperatures (from 300K to 110K). It can be observed that all the resonance spectra exhibit a broad line, centred on g = 2 due to the spin of the Fe^{3+} ions. An additional resonant mode is situated around g = 4.2. By decreasing the temperature the signal around g = 4.2 is well resolved and the signal intensity decreases.

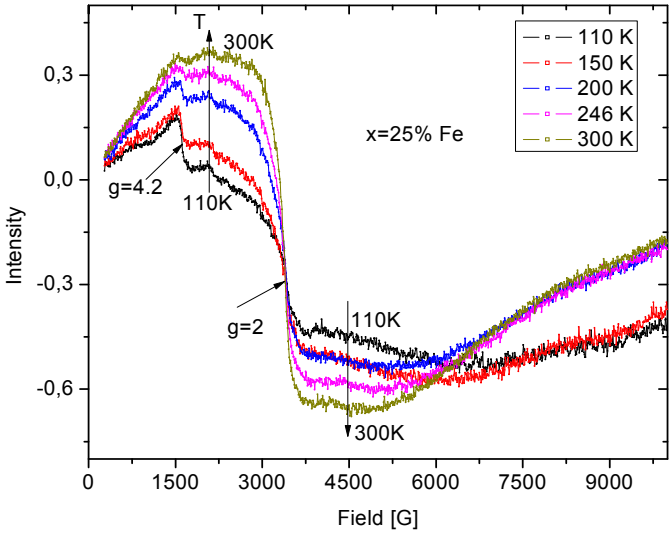

Fig. 1. EPR spectra for x=25 % Fe sample.

The presence of the additional resonant mode is interpreted as an indication of the presence of Fe^{3+} cations in a tetrahedral environment with a strong rhombic distortion.

The complete evolution of the EPR line intensity/concentration of the paramagnetic Fe^{3+} centres with the temperature, as determined in the present investigation, is presented in figure 2. One finds that the EPR line intensity of the Fe^{3+} paramagnetic centre decreases with decreasing temperature. This suggest the increase of the number of antiferromagnetic Fe^{3+}-Fe^{3+} pairs by decreasing temperature.

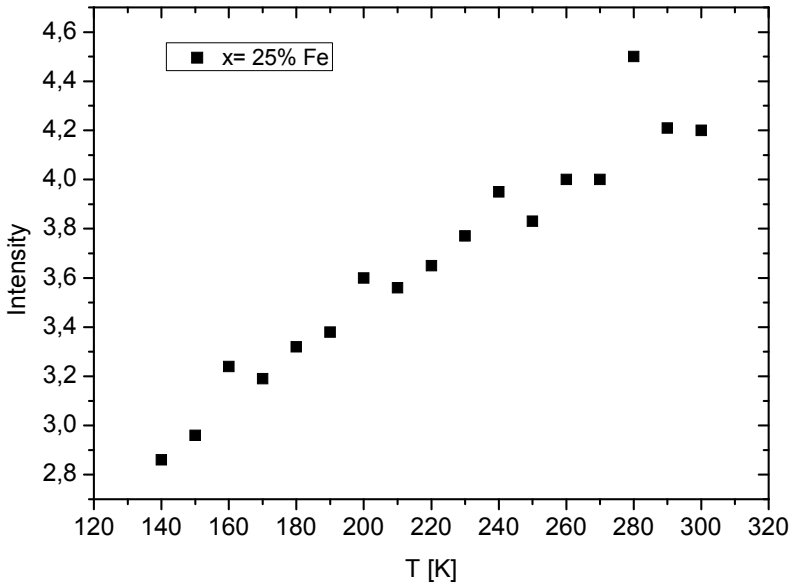

Fig. 2. Temperature dependence of the EPR integrated intensity of the x=25% Fe sample.

Figure 3 shows that the linewidth ΔH_{pp} increases by decreasing temperature. The large value of ΔH_{pp} is the result of a strong magnetic dipolar interaction between the Fe^{3+} ions [20].

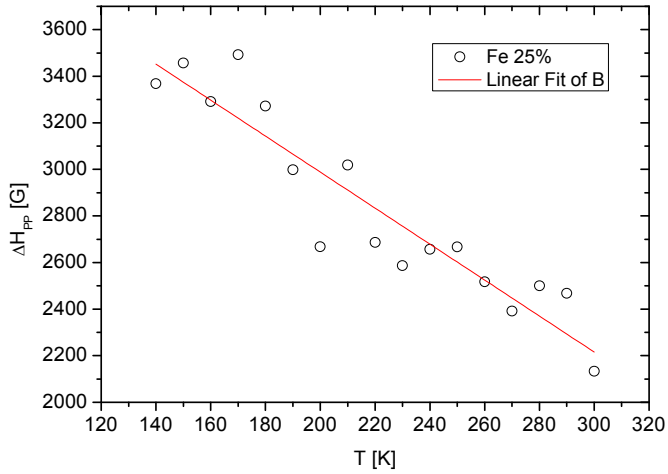

Fig. 3. Temperature dependence of the line width in function of temperature for x=25%Fe sample.

Figure 4 shows that the g-factor increases linearly with decreasing temperature, presenting a change of the slope around ~176 K. The approximate temperature rate of change for the g-factor is $\Delta g/\Delta T \sim 0.17 \cdot 10^{-3}$ K^{-1} in the temperature range of 300 to 180 K and $\Delta g/\Delta T \sim 1.26 \cdot 10^{-3}$ K^{-1} (170 –138 K).

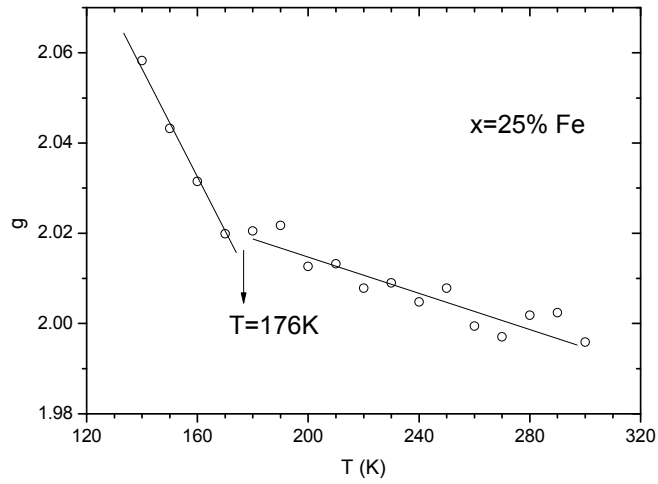

Fig. 4. Temperature dependence of the g–factor for x=0.25 sample.

The double logarithmic plot of linewidth ΔH_{pp} versus a shift of resonance field ΔH_r (see Fig. 5) reveals the existence of two relaxation types with negative slope in the high temperature ranges (300 - 180 K), (175 - 130 K), with a crossover temperature T_s around 175 K.

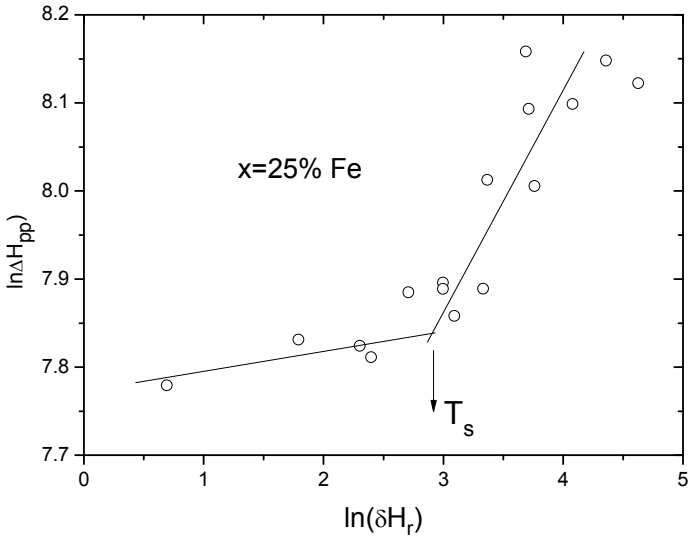

Fig. 5. Plot of $\ln(\Delta H_{pp})$ vs. $\ln(\delta Hr)$ for the x=25% Fe sample. The crossover temperature is indicated by the arrow.

Figure 6 shows the spectra for the x=40% Fe sample at the same 5 temperatures as for x=25% Fe sample. The signal seems to contain two components: a large transition attributed to Fe^{3+} ions (assigned to the central fine structure $\Delta M_S = -1/2 \rightarrow 1/2$ transition) and a hyperfine structure, respectively.

The EPR line intensity of a paramagnetic centre is proportional with its concentration. For the x=40%Fe sample the decrease of the EPR signal with the decreasing temperature shows that the concentration of free Fe^{3+} ions decreases. This behaviour is related with the antiferromagnetic order evidenced from magnetic susceptibility measurements.

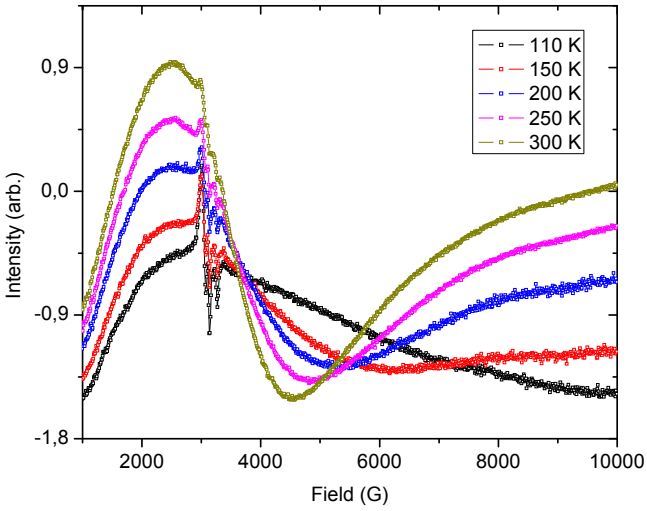

Fig. 6. EPR spectra for the x=40 % Fe sample at different temperatures.

Figure 7 shows that by decreasing the temperature, the hyperfine structure becomes well resolved.

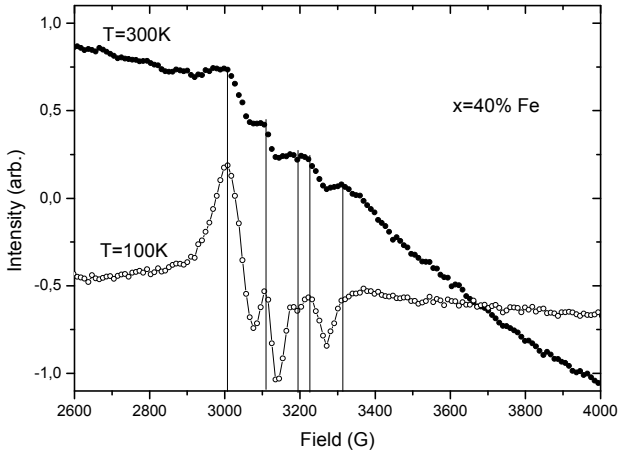

Fig. 7. The hyperfine structure of x=40% Fe sample at temperatures T=300K and T=100K, respectively.

Figure 8 shows that the linewidth ΔH_{pp} increases by decreasing temperature with a slope of $\Delta H_{pp}/\Delta T$ = -6.5 G/K, a value lower comparatively with the one obtained for the x=25% Fe sample ($\Delta H_{pp}/\Delta T$ = -7.7 G/K). The large value of ΔH_{pp} confirms the presence of a strong magnetic dipolar interaction between the Fe^{3+} ions.

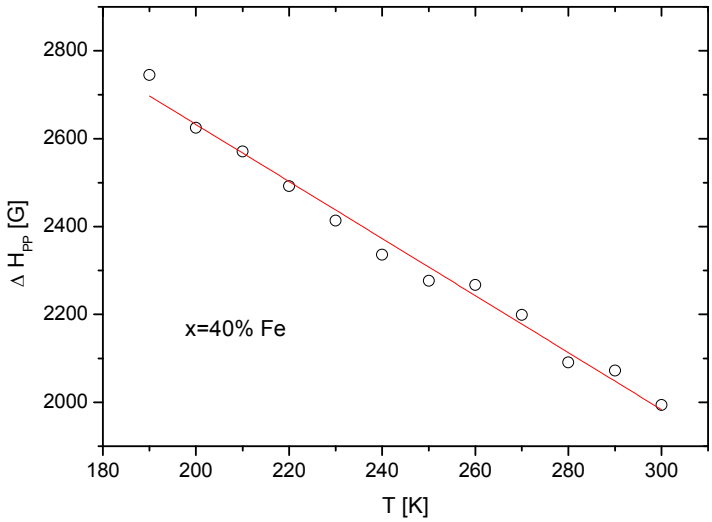

Fig. 8. Temperature dependence of the line width function of temperature for x=40%Fe sample.

Figure 9 shows that the *g*-factor decreases with decreasing temperature, with a noticeable change observed about ~260 K and 200 K. The temperature change for the g-factor is $\Delta g/\Delta T = 1.95*10^{-3}$. The shift of g-factor and the decrease of ΔH_{pp} suggest the increase of the exchange interaction in the sample with x=40% Fe comparatively with the x=25% Fe sample.

The double logarithmic plot of linewidth ΔH_{pp} versus a shift of resonance field ΔH_r (see Fig. 10) shows the existence of a single relaxation type with positive slope in the high temperature range (300-200 K).

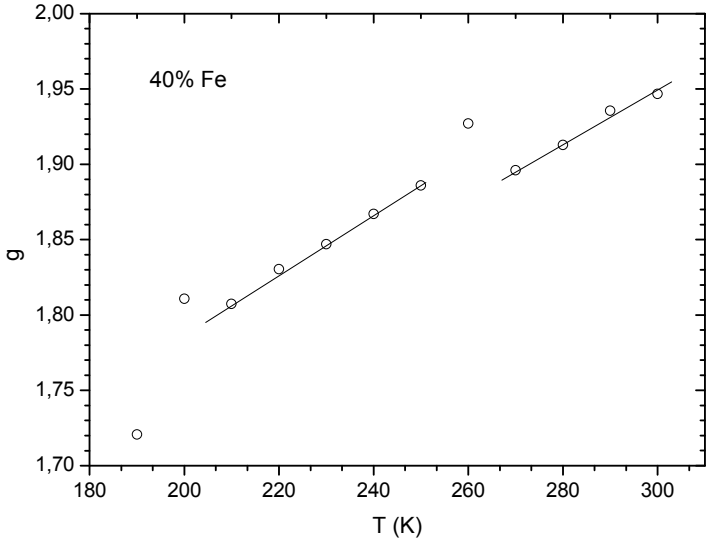

Fig. 9. Temperature dependence of the g – factor for sample x=40% Fe.

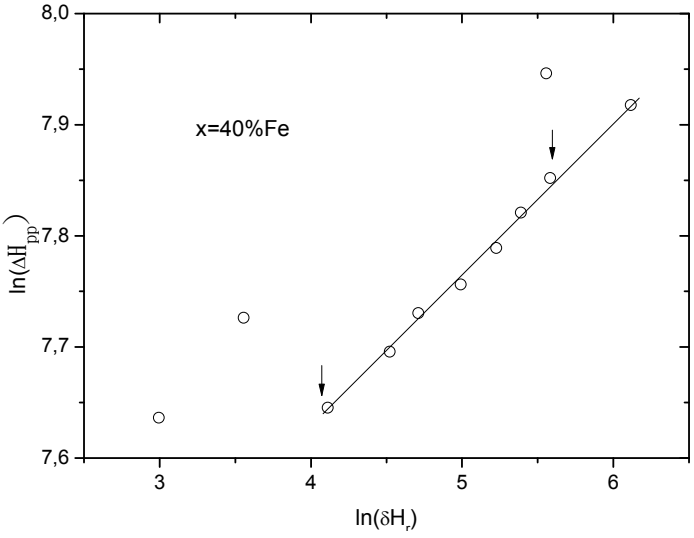

Fig. 10. Plot of $\ln(\Delta H_{pp})$ vs. $\ln(\delta Hr)$ for sample x=40% Fe.

Figure 11 shows comparatively the fine structure of the $PbVO_3$ (x=0.00 Fe) and of x=40% Fe samples. The shift to lower fields of fine structure for x=40% Fe sample (PVF_40) suggest the existence of a different internal field because of the Fe ions. Most likely, the fine structure can be attributed to the vanadium ions.

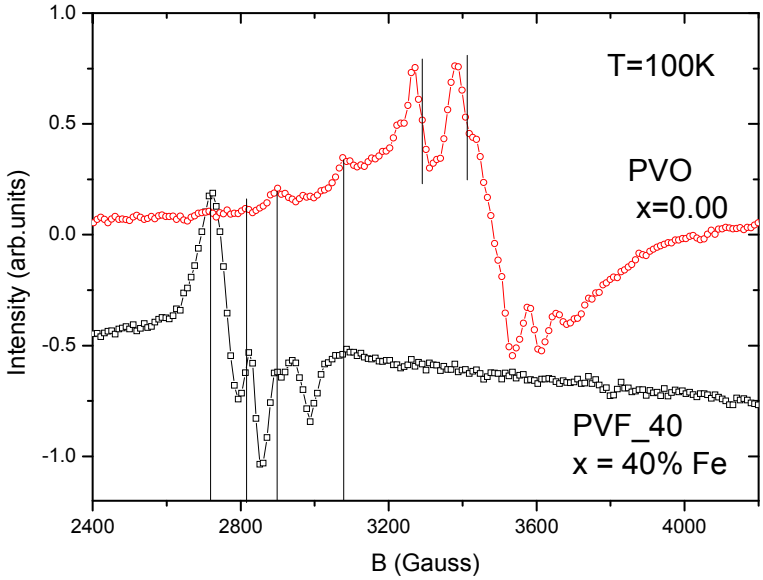

Fig. 11. Hyperfine structure of sample $PbVO_3$ (x=0.0 Fe) and of the x=40%Fe sample.

CONCLUSIONS

EPR results function of temperature for $PbVO_3$ are consistent with the presence of V^{4+} paramagnetic ions in a square–pyramidal C_{4v} coordination (with hyperfine coupling constants $A_{||}$ and $A_{\perp}$),[11]. The evolution of the hyperfine coupling constants function of temperature is in agreement with the small increase of unit cell height c with increase of the temperature [10].

All resonance spectra function of temperature, for samples x=25% and 40% exhibit a broad line, centred on g=2 due to the spin of the Fe^{3+} ions.

For the x = 25%Fe sample, an additional resonant new absorption mode situated around g=4.2 was evidenced. It is attributed of the presence of Fe^{3+} ions on a tetrahedral environment with a strong rhombic distortion.

For sample with x=40% Fe, the superimposed hyperfine structure around g=2 can be attributed to the vanadium ions.

The large value of ΔH_{pp} is the result of strong magnetic dipolar interaction between the Fe^{3+} ions in both the x=25% and 40% Fe samples.

The shift of g-factor and the decrease of ΔH_{pp} suggest the increase of the exchange interaction in sample by increasing x.

The decrease of EPR line intensity attributed to Fe^{3+} paramagnetic centre with decreasing temperature, suggest the increase of the number of antiferromagnetic pairs Fe^{3+}-Fe^{3+}.

For the sample x=25% Fe two relaxation mechanisms were evidenced with a crossover temperature T_s around 175K, while for the x=40% Fe sample only a single relaxation type is present.

REFERENCES

1. Shpanchenko R.V., Chernaya V.V., Tsirlin A.A., Chizhov P.S., Sklovsky D.E. and Antipov E.V., 2004, *Chem. Mater*., 16, 3267-3273.
2. Oka K., Yamada I., Azuma M., Takeshita S., Satoh K.H., Koda A., Kadono R., Takano M. and Shimakawa Y., 2008, *Inorg. Chem*., 47, 7355.
3. Singh D.J., 2006, *Phys. Rev. B*, 73, 094102.
4. Tsirlin A.A., Belik A.A., Shpanchenko R.V., Antipov E.V., Takayama- Muromachi E. and Rosner H., 2008, *Phys. Rev. B,* 77, 092402.
5. Uratani Y., Shishidou T. and Oguchi T., 2009*, J. Phys. Soc. Jpn.,* 78, 084709.

6. Kumar A., Martin L.W., Denev S., Kortright J.B., Suzuki Y., Ramesh R. and Gopalan V., 2007, *Phys. Rev. B*, 75, 060101.
7. Bonner J.C. and Fisher M.E., 1964, *Phys. Rev*., 135, A640.
8. Tsuchiya T., Katsumata T., Ohba T. and Inaguma Y., 2009, J*. Ceram. Soc. Jpn.,* 117, 102.
9. Takeshi Tsuchiya, Tetsuhiro Katsumata, Tomonori Ohba, Yoshiyuki Inaguma, *J. of the Ceramic Society of Japan*, 2009, 117, 102-105.
10. Al. Okos, C. Colin, C. Darie, O. Raita, P. Bordet, A. Pop, 2014, *J. Alloys and Compounds*, 602, 265-268.
11. Al. Okos, A. Pop, Céline Darie, P. Bordet, 2013, *Studia UBB Physica*.
12. O.R. Nascimento, C.J. Magon, L.V.S. Lopes, José Pedro Donoso, E. Benavente, J. Páez, Vladimir Lavayen, María Angélica Santa Ana, G. González, 2006, *Molecular Crystals and Liquid Crystals*, Volume 447, Issue 1.
13. O. Cozar, I. Ardelean, I. Bratu, S. Simon, C. Craciun, L. David. C. Cefan, 2001, *Journal of Molecular Structure*, 563-564.
14. A. Agarwall, A. Sheoran, S. Sanghi, V. Bhatnagar, S.K. Gupta, M. Arora, 2010, *Spectrochimica Acta, Part A*, 75.
15. R.P. Sreekanth Chakradhar, A. Murali, J. Lakshmana Rao, 2000, *Physica B*, 293.
16. N. Vedeanu, O. Cozar, I. Ardelean, V. Ioncu, 2007, *J. Opt. Adv. Mat.*, Vol 9, 844-847.
17. Grommen R., Manikandan P., Geometry and Framework Interactions of Zeolite-Encapsulated Copper(II)-Histidine Complexes, 2000, *J. Am. Chem. Soc.,* 122, 11488-11496.
18. Lin D.H., Coudurier G., Vedrine J., Zeolites: Facts, Figures and Future, Proc 8'th Int. Zeolite Conf., Amsterdam, The Netherlands, July 10–14 1989, Elsevier, Amsterdam*, Stud. Surf. Sci. Catal*., 49, 1431, 1989.
19. Bert M. Weckhuysen, Ralf Heidler, 2004, Electron Spin Resonance Spectroscopy, *Mol. Sieves,* 4, 295–335.
20. John A. Weil, James R. Bolton, and John E. Wertz, 1994, Electron Spin Resonance: Elementary Theory and Practical Applications - John Wiley & Sons, New York.